ISSN 1027-4510, Journal of Surface Investigation: X-ray, Synchrotron and Neutron Techniques, 2017, Vol. 11, No. 2, pp. 474–479. © Pleiades Publishing, Ltd., 2017.
Original Russian Text © A.S. Rysbaev, J.B. Khujaniyozov, I.R. Bekpulatov, A.M. Rakhimov, O.R. Pardaev, 2017, published in Poverkhnost', 2017, No. 4, pp. 98–103.

Effect of Thermal and Laser Annealing on the Atom Distribution Profiles in Si(111) Implanted with P^+ and B^+ Ions

A. S. Rysbaev*, J. B. Khujaniyozov, I. R. Bekpulatov, A. M. Rakhimov, and O. R. Pardaev

Tashkent State Technical University, Tashkent, 100095 Uzbekistan

**e-mail: rysbaev@mail.ru*

Received August 12, 2016

Abstract—The results of studying the effect of thermal and laser annealing on the distribution profiles of phosphorus and boron atoms in Si(111), implanted with different energies and radiation doses, are presented. It is demonstrated that an almost uniform distribution of impurity atoms can be obtained in the near-surface region of Si(111) by means of high-dose ion implantation and thermal and laser annealing. By the phased ion implantation of P^+ and B^+ into different sides of Si(111) with a gradual decrease in energy and radiation dose, *p–i–n* structures with a controlled thickness of the *p* and *n* regions are obtained, which is of great practical importance in the establishment of various device structures.

Keywords: implantation, nanoscale films, surface, single crystal, heterostructure

DOI: 10.1134/S1027451017020318

INTRODUCTION

Over the past decade, nanomaterials have attracted the specific attention of researchers in almost all fields, and the number of publications on this subject is growing exponentially every year [1].

Ion implantation is one way to create nanoscale films in the near-surface region of semiconductors [2]. The properties of thin films are determined by their elemental and chemical composition and the nature of the distribution of an implanted impurity over depth of the initial material.

The aim of this study is to investigate the effect of thermal annealing and infrared and laser radiation on the distribution profiles of phosphorus and boron atoms implanted in Si(111) with different energies and radiation doses.

EXPERIMENTAL

Experimental measurements were carried out in a unit with a spherical-mirror analyzer with a retarding field, enabling investigation of the surface by Auger electron spectroscopy (AES), elastically scattered electron spectroscopy (ESES), photoelectron spectroscopy (PES), and low energy electron diffraction (LEED) at a pressure of residual gases of no greater than 10^{-7} Pa [3, 4]. The objects of the study were single crystals of GaAs, GaP(111), and Si(111) of *n*- and *p* types with a resistivity of 6000 Ω cm. In the chamber, the processes of cleaning the surface of the test materials by heating, electron bombardment, ion etching, and the ion implantation of Ba^+ and alkali metal ions with an energy of 0.5–5 keV, with different doses from 10^{13} to 2×10^{17} cm^{-2}, were carried out. In addition, a clean surface was obtained by cleavage in ultrahigh vacuum. The silicon samples were purified by heating in two phases: long-term heating at 1200 K for 60 min and short-term heating at 1500 K for 1 min. Laser annealing of the ion-implanted samples was performed using a conventional solid state laser of the TRL-403 type with the following operating characteristics: wavelength $\lambda = 1.064$ and 0.532 μm; a pulse width at half maximum of 10–50 ns; a pulse repetition frequency of 10–50 Hz; the energy of laser radiation at a wavelength of 1.064 μm was 0.3–0.4 J and, at a wavelength of 0.532 μm, it was 0.02–0.1 J; a divergence of the laser radiation energy of no larger than 3 mrad (inaccuracy of the pulse energy was 3–5%). Upon the irradiation of the ion-implanted silicon samples, the laser energy density varied from 0.5 to 4 J cm^{-2}. The atom distribution profiles were obtained using stratified surface-layer etching with an Ar^+ ion beam with an energy of 1.5 keV, incident at an angle of 15° to the target surface, and recording of the Auger spectra. The concentration of atoms was estimated by quantitative Auger spectroscopy with matrix corrections [5].

RESULTS AND DISCUSSION

Our experiments showed that after the implantation of P^+ and B^+ ions into Si(111) with a large dose $D > 10^{16}$ cm^{-2} in the near-surface region, the thickness of which depends on the energy of the implanted ions, a layer is formed with a substantially uniform distribu-

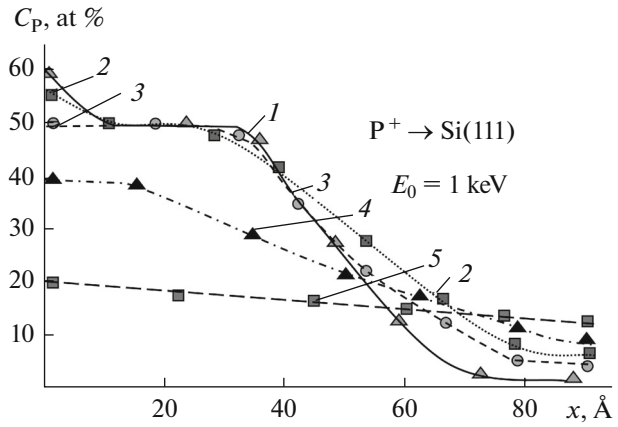

Fig. 1. Concentration distribution profiles of phosphorus atoms implanted into Si(111) with the energy $E_0 = 1$ keV over depth x, obtained after short-term thermal annealing at various temperatures T: (*1*) 300, (*2*) 600, (*3*) 1000, (*4*) 1200, and (*5*) 1300 K.

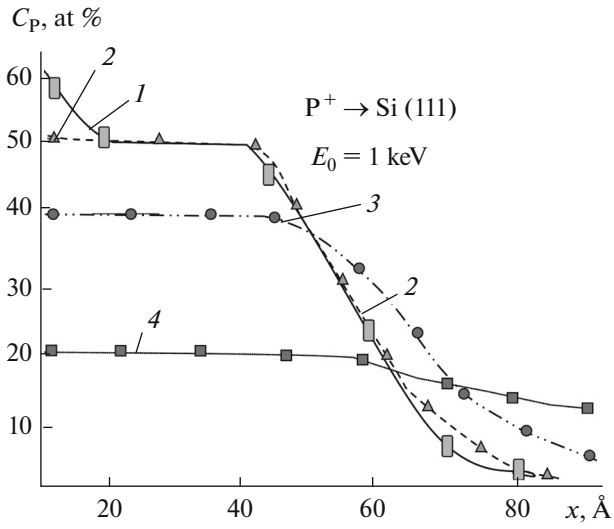

Fig. 2. Concentration distribution profiles of phosphorus atoms implanted into Si(111) with the energy $E_0 = 1$ keV over depth x, obtained after pulsed laser annealing at various energy density W: (*1*) 0, (*2*) 1.0, (*3*) 2.5, and (*4*) 4 J cm^{-2}.

tion of impurity atoms, some of which form a chemical compound with silicon atoms. However, in the ion-implantation process, together with the accumulation of impurities, various defects are formed, and the ion-implanted layer becomes amorphous [6]. Therefore, to obtain layers with certain stable properties and to heal defects, postimplantation annealing is required. In the implantation of P^+ and B^+ ions with low doses of $D \le 10^{13}$ cm^{-2} into silicon, annealing is carried out to heal defects and transferimpurity atoms into an electrically active state. In this case (in the implantation of P^+ and B^+ with high doses of $D > 10^{16}$ cm^{-2}), annealing, except for the healing of defects, is carried out to convert all of the implanted atoms into a chemically bound state to synthesize a new chemical compound. At the same time, in our opinion, the rapid formation of silicide compounds is observed near the (amorphouslayer)–(single crystal) interface. The postimplantation annealing of defects is usually carried out thermally by heating, infrared (IR) radiation, or laser radiation. The last two methods have a number of advantages compared to thermal annealing, which consist in localization of the thermal effect of radiation; annealing can be performed in the pulsed mode, and the effect of the thermal field on the temperature of the surrounding elements is lacking. The annealing of ion-implanted samples was carried out in high vacuum (~10^{-6}–10^{-7} Pa). The procedure of thermal annealing by heating and laser and infrared radiation is described in detail in [7].

Figure 1 shows how the changes that occur in the concentration distribution profile of phosphorus atoms implanted into silicon with the energy $E_0 = 1$ keV and dose $D = 1 \times 10^{17}$ cm^{-2} after thermal heating at different temperatures. It is seen from the figure that the heating of ion-implanted silicon at $T = 600$ K leads to a decrease in the concentration of phosphorus atoms C_P on the surface to 55 at %, which is probably due to the desorption of phosphorus atoms. At the same time, only a small fraction, 5–8 at %, of phosphorus atoms diffuse into bulk silicon at this temperature. After short-term heating at $T = 1000$ K, the concentration of phosphorus atoms in a near-surface region of thickness x ~ 30 Å is ~50 at %, which corresponds to the formation of silicon phosphide SiP with a single-crystal structure. At $T > 1000$ K, intense diffusion of phosphorus atoms into the sample is observed, which increases the width of the transition layer.

At $T = 1200$–1300 K, along with diffusion, breaking of the chemical bond between silicon and phosphorus atoms and desorption of the latter from the surface area are observed; heating at $T = 1350$ K causes the complete electrical activation of phosphorus atoms. We also recorded the distribution profiles of phosphorus atoms in the silicon samples implanted with P^+ ions with an energy of $E_0 = 1$ keV at a dose of $D = 1 \times 10^{17}$ cm^{-2} and subjected to pulsed laser annealing (with the wavelength $\lambda = 1.064$ μm and a pulse duration of ~10 ns) with differing energy density W (Fig. 2): (*1*) 0, (*2*) 1.0, (*3*) 2.5, and (*4*) 4 J cm^{-2}.

Pulsed laser annealing with $W \le 1.0$ J cm^{-2} yields an almost stepwise distribution of phosphorus atoms. In this case, a compound of SiP is formed in a near-surface region with the thickness 35–40 Å. Increasing the laser energy density leads to decomposition of the SiP compound and a decrease in the concentration to 40 at % (at $W = 2.5$ J cm^{-2}) and 20 at % (after annealing at $W = 4$ J cm^{-2}). The comparison of thermal and laser annealing (Fig. 1, curve *2* and Fig. 2, curve *2*) shows that laser annealing yields a sharper distribution pro-

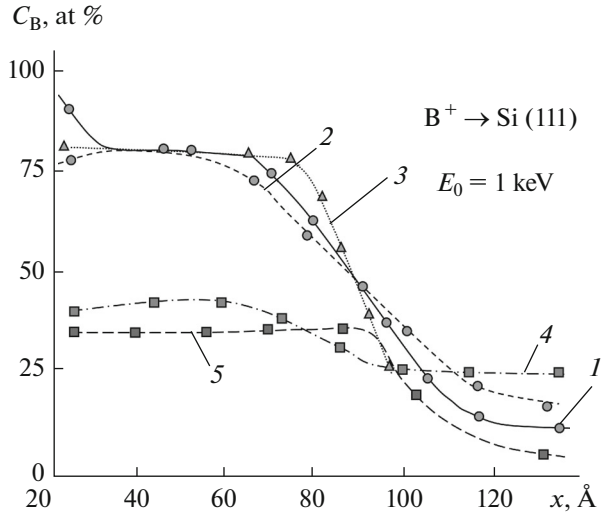

Fig. 3. Concentration distribution profiles of boron atoms implanted into Si(111) with the energy E_0 = 1 keV over depth x, obtained after thermal annealing at (*1*) 300, (*2*) 900, and (*4*) 1200 K and laser annealing at an energy density W of (*3*) 1.0 and (*5*) 3 J cm^{-2}.

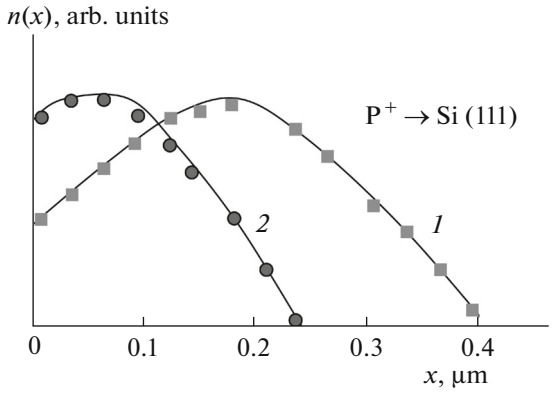

Fig. 4. Distribution profiles of phosphorus atoms over depth x, implanted into Si(111) with (*1*) energy E_0 = 80 keV and dose $D = 1.8 \times 10^{16}$ cm^{-2} and (*2*) E_0 = 20 keV and $D = 1.8 \times 10^{15}$ cm^{-2}.

file of phosphorus atoms with a smaller width of the transition region SiP–Si than thermal annealing.

The pulsed laser annealing of Si(111) implanted with B+ ions at W = 1.0 J cm^{-2}, as well as in the case of P^+ ions, leads to the heterostructural transition SiB_3–Si with a fairly sharp interface (Fig. 3, curve *3*). For the decomposition of chemical compound SiB_3 and complete electrical activation of the remaining boron atoms, thermal heating at T = 1200 K or laser annealing at W = 3 J cm^{-2} is required. We note that after laser annealing of the ion-implanted samples, an n^-–p junction is formed in the case of phosphorus, and p^{++}–p junction is observed in the case of boron.

In addition, we also studied the distribution profiles of phosphorus and boron atoms implanted in Si(111) with a higher energy: 10, 20, and 80 keV. In this case, the annealing of ion-implanted samples was performed by heating and pulsed infrared irradiation with a wavelength of λ = 1 μm and a pulse duration on the order of microseconds. The investigation of changes in the distribution profiles for phosphorus and boron atoms implanted with different energies by means of thermal and pulsed IR annealing showed that annealing using infrared radiation, as laser annealing, yields sharper profiles of implanted atoms than thermal annealing. It is obvious that at these ion energies, even at high doses, the concentration of impurity atoms is much less than the concentration of silicon atoms. However, this does not mean that a chemical interaction between atoms is impossible [8].

The distribution profiles of phosphorus and boron atoms implanted into silicon at different radiation doses $D \approx 1 \times 10^{13}$–$1 \times 10^{17}$ cm^{-2} were studied, recorded before and after annealing with IR radiation. Based on this analysis, we determined the optimal energy and radiation doses and the conditions of subsequent annealing to obtain the highest possible concentration of electrically active impurities of phosphorus and boron with their uniform distribution over sample depth. It was found that to obtain a uniform distribution of phosphorus atoms in Si(111), it is necessary to carry out the sequential implantation of P^+ ions, first, with an energy of E_0 = 80 keV and a dose of $D = 1.8 \times 10^{16}$ cm^{-2} (Fig. 4) and then with E_0 = 20 keV and $D = 1.8 \times 10^{15}$ cm^{-2}. IR annealing should be conducted after each ion-implantation stage.

In the case of boron, the optimal conditions for implantation and annealing are as follows: first, the implantation of B^+ ions with E_0 = 80 keV and $D = 0.9 \times 10^{16}$ cm^{-2}, then with E_0 = 20 keV and $D = 3 \times 10^{15}$ cm^{-2}, and finally with E_0 = 10 keV and $D = 1.8 \times 10^{15}$ cm^{-2}; annealing by IR radiation should also be conducted after each ion-implantation stage (Fig. 5). As seen from Figs. 4 and 5, ion implantation and subsequent annealing performed as described above give a substantially uniform distribution of phosphorus atoms in a layer with the thickness $x \approx 0.4$ μm, and boron atoms in a layer with $x \approx 0.6$ μm. The modes of ion implantation and subsequent annealing, selected for electrical activation, ensured a stepwise distribution of phosphorus and boron atoms and a sharp interface between the impurity region and the silicon base region. AES estimation of the concentration of electrically active atoms indicates that $N_P = 10^{21}$ cm^{-3} and $N_B = 2 \times 10^{21}$ cm^{-3}. Similar results are obtained if laser pulsed annealing with an energy density of W = 3 J cm^{-2} (wavelength λ = 1.064 μm, pulse duration ~10 ns) is performed after each stage of ion implantation. That is, such ion implantation can yield a p–i–n structure with a high concentration of electrically active impurities and a sharp boundary

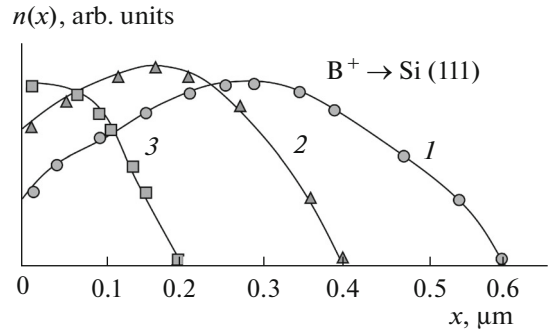

Fig. 5. Distribution profiles of boron atoms over depth x, implanted into Si(111) with (*1*) energy $E_0 = 80$ keV and dose $D = 0.9 \times 10^{16}$ cm^{-2}, (*2*) $E_0 = 25$ keV and $D = 3 \times 10^{15}$ cm^{-2}, and (*3*) $E_0 = 10$ keV and $D = 1.8 \times 10^{15}$ cm^{-2}.

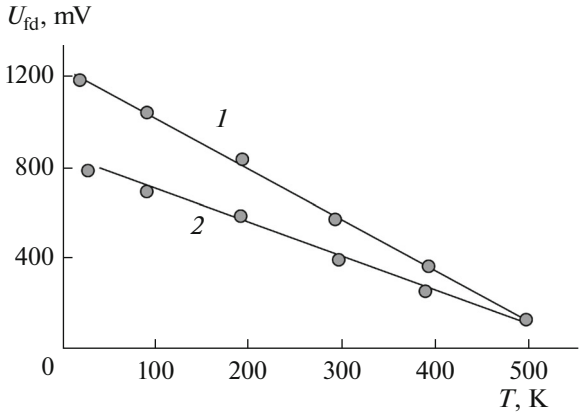

Fig. 6. Dependence of the forward voltage drop across the p–i–n junction on the heating temperature for Si(111) with a resistivity of ρ = (*1*) 6000 and (*2*) 3000 Ω cm.

between the p–i and i–n regions of silicon. We note that a large concentration of carriers in the p and n regions of silicon is also necessary to smooth the temperature dependence of the contact area of devices based on a p–i–n junction. The LEED study of the crystal structure of Si(111) surfaces after the above ion implantation and subsequent annealing showed that both surfaces of the p–i–n junction had single-crystalline structure.

The thus obtained p–i–n structure is a diode with p-type conductivity of the base i-region. To examine the current–voltage characteristics of the p–i–n diode, metallic contacts were applied to both surfaces of the crystal. The diode surface was metallized by the vacuum deposition of nickel and titanium atoms at a substrate temperature of $T = 600$ K. Titanium atoms were deposited first, and then nickel atoms. The TiNi film thickness on the surfaces of the p–i–n structure was 200 Å.

Investigation of the dependence of the forward voltage drop U_{fd} on temperature during the formation of the p–i–n structure by the implantation of P^+ and B^+ ions into silicon with a gradual decrease in the ion energy and dose and pulse annealing showed that after the first stage of ion implantation, the dependence $U_{fd} = f(T)$ is nonlinear. After the second stage of ion implantation and annealing, the dependence $U_{fd} = f(T)$ becomes linear at low temperatures (≤250 K), while after the third stage of ion implantation and annealing, this dependence becomes linear throughout the entire temperature range. We note that the dependences shown in Fig. 6 are obtained by passing current $I_n = 1$ mA through the p–i–n structure and its connection to the circuit in the mode of constant current (I_n = const). It is seen (Fig. 6) that the operating characteristics of the sensor also depends on the resistivity ρ of the initial silicon, that is, it is determined by processes in the base region of the p–i–n diode. With decreasing ρ of initial silicon, the sensor sensitivity somewhat decreases.

Thus, the above process conditions of ion implantation and pulsed infrared annealing are optimal for producing a temperature sensor having the following parameters [9]: (1) the measured temperature range is from 20 to 500 K, and in the entire temperature range the dependence $U_{fd} = f(T)$ is linear; (2) the temperature sensitivity is 2.1 mV K^{-1}; and (3) the supply current is from 100 μA to 1 mA.

The annealing of defects by heating, laser irradiation, or infrared light results, along with a variation in the distribution profile of phosphorus and boron

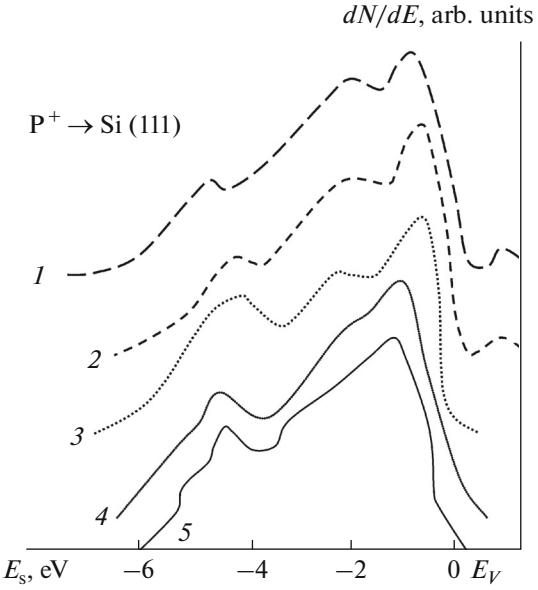

Fig. 7. Photoelectron spectra of Si(111) implanted with P^+ ions with $E_0 = 1$ keV, recorded after heating at different temperatures T: (*1*) 300, (*2*) 900, (*3*) 1000, (*4*) 1200, and (*5*) 1550 K.

Electron energy parameters of silicon implanted with P^+ and B^+ ions, obtained after subsequent thermal annealing in different modes

Electron energy parameters	Annealing temperature T, K									
	$P^+ \rightarrow Si(111)$					$B^+ \rightarrow Si(111)$				
	300	900	1000	1300	1550	300	600	900	1300	1550
Thermionic work function $e\varphi$, eV	3.1	3.2	3.5	4.5	4.7	3.6	4.0	4.7	4.7	4.7
Band gap E_g, eV	0.8	1.0	1.45	1.2	1.1	0.9	1.1	1.3	1.2	1.1
Photoelectron work function Φ, eV	3.8	4.2	4.9	5.0	5.1	3.8	4.2	4.8	5.0	5.1
Electron affinity χ, eV	3.0	3.2	3.45	3.8	4.0	2.9	3.1	3.5	3.8	4.0

atoms, to a change in the chemical state of atoms and alters the electronic structure of the near-surface region of ion-implanted Si(111).

Figure 7 presents the photoelectron spectra (PES) for Si(111) implanted with P^+ ions with the energy $E_0 = 1$ keV, recorded after different thermal heating at (*1*) 300, (*2*) 900, (*3*) 1000, and (*4*) 1550 K. It is seen that the thermal heating of ion-implanted silicon leads to a significant change in the photoelectron spectra; the intensity and shape of some peaks changes; a decrease in the width of the spectrum is observed; and new maxima appear. For example, heating at $T = 900$ K increases the intensity and shifts the maximum at $E_s = -0.6$ eV to higher energies, which allows this maximum to be attributed to compound SiP. A decrease in the intensity of the peak at $E_s = +0.8$ eV is obviously caused by a decrease in the concentration of unbound phosphorus atoms due to their partial desorption and the formation of Si–P bonds.

Spectrum *3* (Fig. 7) obtained after annealing at $T = 1000$ K reflects the density of states of valence electrons of silicon phosphide. At this temperature, the peak at $E_s = +0.8$ eV associated with the impurity subband disappears, indicating the absence (within error of changes) of unbound phosphorus atoms. A further increase in the annealing temperature leads to partial decomposition of the Si–P bonds and the desorption of phosphorus atoms from the near-surface region. After heating at $T = 1550$ K, the photoelectron spectrum (curve *5*) is virtually identical to the spectrum of the pure surface of Si(111). Similar changes occurred in the photoelectron spectra after heating silicon implanted with boron ions. The table shows the values of the electron energy parameters of silicon implanted with P^+ and B^+ ions, obtained after subsequent thermal annealing in different modes.

It is seen from the Table that postimplantation thermal annealing leads to a change in the parameters of the energy bands of the ion-implanted silicon samples. In the case of Si(111) implanted with P^+ ions, heating to 1000 K results in the formation of SiP compound, and in the case of Si(111) implanted with B^+ ions, the formation of the SiB_3 compound occurs after heating at $T = 900$ K. The subsequent heating of the samples at higher temperatures of $T \geq 1200$ K causes the decomposition of these compounds and the desorption of impurity atoms into vacuum, which is accompanied by approximation of the band energy parameters to the corresponding values of pure silicon.

CONCLUSIONS

Thus, it is found in the work that the implantation of P^+ and B^+ ions into Si(111) with an energy of 1 keV and a dose of 10^{17} cm^{-2} and subsequent thermal or laser annealing can yield an almost stepwise distribution of impurities in the near-surface region with the thickness 35–40 Å. Laser annealing ensures that a sharper distribution profile of phosphorus atoms with a smaller width of the transition region of SiP–Si than in the case of thermal annealing is obtained.

By the phased implantation of P^+ and B^+ ions on different sides of Si(111) with a gradual decrease in energy and radiation dose, *p–i–n* structures with a controlled thickness of the *p* and *n* regions are obtained, which is of great practical importance in the development of various device structures. Optimal modes of implantation and annealing are determined to obtain a temperature sensor based on single-crystal silicon, having a high sensitivity and linear response over a broad temperature range.

ACKNOWLEDGMENTS

This work was financially supported by the State Fundamental Science Program, project no. F-2-31 RUz.

REFERENCES

1. A. S. Rysbaev, *Thin Nanosized Silicide Films: Synthesis and Properties* (Tashkent State Technical Univ. Named after Abu Rayhon Beruni, Tashkent, 2013) [in Russian].
2. I. P. Suzdalev, *Nanotechnology: Physical Chemistry of Nanoclusters, Nanostructures and Nanomaterials* (Komkniga, Moscow, 2006) [in Russian].
3. A. S. Rysbaev, M. T. Normuradov, Yu. Yu. Yuldashev, et al., J. Commun. Technol. Electron. **42**, 220 (1997).
4. M. T. Normuradov, D. S. Rumi, and A. S. Rysbaev, Izv. Akad. Nauk UzSSR, Ser. Fiz.-Mat. Nauk, No. **4**, 70 (1986).
5. A. K. Tashatov, Doctoral Dissertation in Mathematics and Physics (Institute of Electronics Acad. Sci. Resp. Uzbekistan, Tashkent, 2005).
6. A. S. Rysbaev, Zh. B. Khuzhaniyazov, A. M. Rakhimov, et al., Tech. Phys. **59** (10), 1526 (2014).
7. A. S. Rysbaev, Doctoral Dissertation in Mathematics and Physics (Institute of Electronics Acad. Sci. Resp. Uzbekistan, Tashkent, 2003).
8. A. S. Rysbaev, Zh. B. Khuzhaniyazov, M. T. Normuradov, et al., Tech. Phys. **59** (11), 1705 (2014).
9. A. S. Rysbaev, Yu. Yu. Yuldashev, Zh. B. Khuzhaniyazov, and A. M. Rakhimov, UZ Patent No. IAP 04779, Byull. Izobret., No. 6 (2013).

Translated by O. Zhukova